Quasiexact Kondo Dynamics of Fermionic Alkaline-Earth-Like Atoms at Finite Temperatures

Shimpei Goto* and Ippei Danshita†
Department of Physics, Kindai University, Higashi-Osaka City, Osaka 577–8502, Japan

(Received 23 June 2019; published 3 October 2019)

A recent experiment has observed the antiferromagnetic interaction between the ground state $^1S_0$ and the metastable state $^3P_0$ of ^{171}Yb atoms, which are fermionic. This observation combined with the use of state-dependent optical lattices allows for quantum simulation of the Kondo model. We propose that in this Kondo simulator the anomalous temperature dependence of transport, namely, the Kondo effect, can be detected through quench dynamics triggered by the shift of a trap potential. For this purpose, we improve the numerical efficiency of the minimally entangled typical thermal states (METTSs) algorithm by applying additional Trotter gates. Using the improved METTSs algorithm, we compute the quench dynamics of the one-dimensional Kondo model at finite temperatures quasiexactly. We find that the center-of-mass motion exhibits a logarithmic suppression with a decrease in the temperature, which is a characteristic feature of the Kondo effect.

DOI: 10.1103/PhysRevLett.123.143002

Orbital degrees of freedom are a fundamental element for understanding physics of various condensed matter systems, including heavy-fermion materials [1,2], transition metal oxides [3–5], iron pnictides [6–8], and compound semiconductors [9,10]. In these systems, the multiorbital character, together with the spin degrees of freedom and strong interparticle interactions, leads to the emergence of magnetism, superconductivity, excitonic condensation, and the Kondo effect. It is widely believed that the essence of some of these properties can be extracted by analyzing the two-orbital Anderson- and Kondo-type models, in which delocalized fermions in one orbital exchange their spins with localized fermions in the other orbital. However, accurate simulation of these models with classical resources is, in general, intractable because of the exponential growth of the Hilbert space and the minus sign problem in quantum Monte Carlo simulations.

An alternative approach for analyzing the prototypical two-orbital models is analog quantum simulation [11], using optical lattices loaded with ultracold gases [12–14]. It has been proposed that optical-lattice quantum simulators (OLQSs) of the two-orbital models can be realized with the use of fermionic alkaline-Earth-like atoms (AEAs) [15–19], such as strontium [20] and ytterbium [21,22]. A remarkable advantage of AEAs over alkali atoms is the existence of the electronically excited state $^3P_0$ or $^3P_2$ with a long lifetime, which can be coupled to the ground state $^1S_0$ via an ultranarrow clock transition. Riegger *et al.* indeed have used a state-dependent optical lattice to create a two-orbital fermionic quantum gas of ^{173}Yb [23], in which atoms in the $^1S_0$ ($^3P_0$) state play a role of delocalized (localized) fermions. Moreover, Ono *et al.* have reported the observation of antiferromagnetic spin-exchange interaction between the $^1S_0$ and $^3P_0$ states of ^{171}Yb [24]. Since ^{171}Yb atoms in the $^1S_0$ state hardly interact with each other [25], their two-orbital system in a state-dependent optical lattice naturally simulates the Kondo model.

One of the most important targets of the OLQS of the Kondo model is the Kondo effect [26–31], in which a localized fermion forms a many-body spin-singlet state with delocalized fermions when the temperature is lowered. The formation of such Kondo singlets causes the anomalous increase of the resistance with a decrease in the temperature. The Kondo effect is thought to be a key concept for understanding rich quantum phases and phase transitions of the Kondo lattice model represented by a Doniach phase diagram [32]. Since transport properties of trapped quantum gases have been often investigated by measuring their center-of-mass (c.m.) motion induced in response to a sudden displacement of the trapping potential [33–39], it is likely that the Kondo effect in the OLQS of the Kondo model will be detected via such simple transport measurements. However, accurate theoretical predictions on the c.m. dynamics have never been made because of the difficulties in calculating real-time evolution of the quantum many-body system with two orbitals at finite temperatures.

In this Letter, we develop a numerical method that overcomes such difficulties in order to show that the Kondo effect of the Kondo OLQS can be indeed detected by measuring the c.m. motion of the delocalized fermions after the trap displacement. Specifically, we restrict ourselves to one-dimensional (1D) systems, in which matrix product states (MPSs) serve as an efficient description of

states with relatively low energy [40–42], and modify the finite-temperature algorithm using the minimally entangled typical thermal states (METTSs) [43,44]. Our modified METTSs algorithm includes additional Trotter gates and allows for efficient simulations of systems with an Abelian symmetry, such as the Hubbard and Kondo models. Using the modified METTSs, we compute the finite-temperature dynamics of the Kondo model with the antiferromagnetic interaction and find that, when the temperature decreases, the maximum c.m. speed during the dynamics logarithmically decreases; i.e., the transport exhibits a logarithmic suppression, which is a characteristic feature of the Kondo effect. We also analyze the fully spin-polarized system and the ferromagnetic Kondo model, in which the Kondo effect does not occur [45], as references to be compared with the antiferromagnetic case. The logarithmic suppression of the transport is found to be absent in these two cases.

Model and method.—We consider an ultracold mixture of ^{171}Yb atoms, which are fermionic, in the $^1S_0$ and $^3P_0$ states confined in a combined potential of optical lattices and a parabolic trap. We assume that the transverse optical lattice is sufficiently deep such that the system can be regarded to be spatially 1D. The longitudinal optical lattice is state dependent in a way that an atom in the $^3P_0$ state is localized at $j = 0$, while the lattice for $^1S_0$ atoms is modestly deep for the tight-binding approximation to be valid, but is shallow enough to make $^1S_0$ atoms delocalized. This system is well described by the 1D Kondo model [26,46] with a parabolic trap term

$$\hat{H} = -J\sum_{i=-L}^{L-1}\sum_{\sigma}\left(\hat{c}^{\dagger}_{i\sigma}\hat{c}_{i+1\sigma} + \text{H.c.}\right) + V\hat{\boldsymbol{s}}_{i=0}\cdot\hat{\boldsymbol{S}}_{\text{imp}} + w\sum_{i=-L}^{L}\sum_{\sigma}(i - x_c/a)^2\hat{n}_{i\sigma} \tag{1}$$

and can be regarded as an OLQS of the model. The total number of sites is $2L+1$. Here, $\hat{c}^{\dagger}_{i\sigma}$ ($\hat{c}_{i\sigma}$) creates (annihilates) a $^1S_0$ fermion with spin σ at site i, and $\hat{n}_{i\sigma} = \hat{c}^{\dagger}_{i\sigma}\hat{c}_{i\sigma}$. $\hat{\boldsymbol{s}}_i = (\hat{s}^x_i, \hat{s}^y_i, \hat{s}^z_i)$ are spin operators of a $^1S_0$ fermion at site i and each component is defined as $\hat{s}^{\gamma} = (1/2)\sum_{\alpha\beta}\hat{c}^{\dagger}_{i\alpha}\sigma^{\gamma}_{\alpha\beta}\hat{c}_{i\beta}$ with the Pauli matrices $\boldsymbol{\sigma}^{\gamma}$. $\hat{\boldsymbol{S}}_{\text{imp}} = (\hat{S}^x_{\text{imp}}, \hat{S}^y_{\text{imp}}, \hat{S}^z_{\text{imp}})$ are spin operators of the impurity fermion at site 0. J denotes the hopping amplitude of $^1S_0$ fermions, V the spin-exchange interaction between $^1S_0$ and $^3P_0$ fermions, w the amplitude of the trap, x_c the position of the trap center, and a the lattice constant.

The interaction between ^{171}Yb atoms in the $^1S_0$ state can be safely ignored because it is very small (the s-wave scattering length is $a_s = -0.15$ nm [25]). It is worth noting that there exists direct interaction between $^1S_0$ and $^3P_0$ fermions, which is given by $V_d(\sum_{\sigma}\hat{n}_{i=0\sigma})\hat{n}_{\text{imp}}$ [24]. Since the number of a $^3P_0$ fermion $\hat{n}_{\text{imp}}$ is fixed to be unity, the direct interaction is equivalent to a barrier potential at site 0. We assume that a laser beam is focused on site 0 to cancel the direct interaction. Such control can be made in experiment, e.g., by using a digital micromirror device [47,48]. With this Hamiltonian (1), we calculate the time evolution of the c.m. position $\hat{x}_G = \sum_{i=-L,\sigma}^{L} ia\hat{n}_{i\sigma}/N$ with the total particle number of $^1S_0$ fermions $N = \sum_{i\sigma}\langle\hat{n}_{i\sigma}\rangle$ and the c.m. velocity $\hat{v}_G = -(i/\hbar)[\hat{x}_G, \hat{H}]$, followed by the shift of a trap center x_c from $3a$ to 0 at finite temperatures as depicted in Fig. 1.

In order to numerically simulate dynamics of quantum many-body systems at finite temperatures, we use MPSs and the METTSs algorithm. There is another option for computing such finite-temperature dynamics, namely, the purification method [49–52]. However, since in the purification method the density matrix of a system is represented as a pure state by squaring the dimensions of local Hilbert spaces, it is not very efficient for our two-orbital system with large local Hilbert spaces.

In the METTSs algorithm, the thermal expectation value at an inverse temperature $\beta = 1/k_BT$ is calculated as

$$\langle\hat{O}\rangle_{\beta} = \frac{\text{Tr}[e^{-\frac{\beta}{2}\hat{H}}\hat{O}e^{-\frac{\beta}{2}\hat{H}}]}{Z} = \sum_i \frac{\langle i|e^{-\beta\hat{H}}|i\rangle}{Z}\frac{\langle i|e^{-\frac{\beta}{2}\hat{H}}\hat{O}e^{-\frac{\beta}{2}\hat{H}}|i\rangle}{\langle i|e^{-\beta\hat{H}}|i\rangle}, \tag{2}$$

and the summation over orthonormal basis $|i\rangle$ is performed by the Markov-chain Monte Carlo (MCMC) sampling. In the ordinary METTSs algorithm [43,44], the transition probability of the MCMC method from a state $|i\rangle$ to $|j\rangle$ is given by

$$p_{i\to j} = \frac{|\langle j|e^{-\frac{\beta}{2}\hat{H}}|i\rangle|^2}{\langle i|e^{-\beta\hat{H}}|i\rangle}. \tag{3}$$

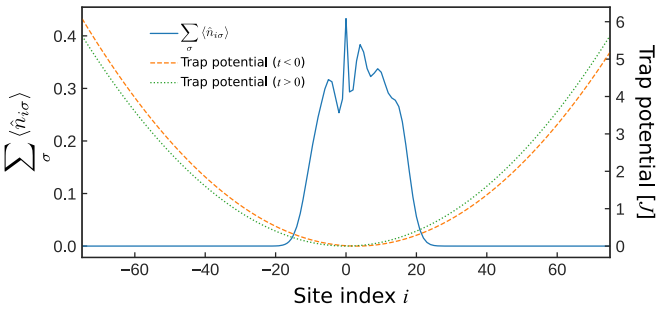

FIG. 1. The solid line represents the density distribution of the delocalized fermions of the Kondo model in the stationary state for $N = 9$, total magnetization $M = 0$, $V/J = 1$, $x_c = 3a$, and $\beta J = 75$. The localized fermion is located at $i = 0$. The dashed and dotted lines represent the parabolic trap potential before and after the displacement of its center.

With this transition probability, the METTSs algorithm suffers from a severe autocorrelation problem at high temperatures, as easily inferred from the $\beta \to 0$ limit. This autocorrelation problem can be eliminated by breaking the total particle number conservation. However, the breaking of the conservation of particle number leads to significant increase of computation time in dynamics. Hence, we introduce the following transition probabilities for odd steps,

$$p_{i\to j}^{\mathrm{odd}} = \frac{|\langle j|[\hat{U}(\tau)]^n e^{-\frac{\beta}{2}\hat{H}}|i\rangle|^2}{\langle i|e^{-\beta\hat{H}}|i\rangle} \tag{4}$$

and

$$p_{i\to j}^{\mathrm{even}} = \frac{|\langle j|e^{-\frac{\beta}{2}\hat{H}}[\hat{U}^\dagger(\tau)]^n|i\rangle|^2}{\langle i|[\hat{U}(\tau)]^n e^{-\beta\hat{H}}[\hat{U}^\dagger(\tau)]^n|i\rangle} \tag{5}$$

for even steps. Here, τ is a parameter that characterizes the Trotter gates,

$$\hat{U}(\tau) = e^{-i\tau\hat{H}_{\mathrm{even}}}e^{-i\tau\hat{H}_{\mathrm{odd}}}, \tag{6}$$

and n is an integer. For $\hat{H}_{\mathrm{even}}$ and $\hat{H}_{\mathrm{odd}}$, one can take any Hermitian operators as long as they respect the conservation of the particle number. We use the products of local Hilbert states in some symmetric sector as the orthonormal basis $|i\rangle$. This approach is a variant of the symmetric METTSs algorithm [53] with symmetric bases $|i\rangle$ and $[\hat{U}^\dagger(\tau)]^n|i\rangle$, which are very flexible because of the parameter τ and the freedom to choose $\hat{H}_{\mathrm{even}}$ and $\hat{H}_{\mathrm{odd}}$. Moreover, the implementation of our approach is quite easy since it requires only the applications of the Trotter gates in addition to the ordinary METTSs algorithm. With the transition probabilities, we can reduce the autocorrelation time by increasing τ and n without breaking the conservation. However, since the bond dimensions of MPSs increase with τ and n, some tuning of the parameters may be required for efficient simulations. The validity of our approach and some benchmark results are shown in the Supplemental Material [54].

The dynamics of the thermal expectation value is obtained by representing the operator $\hat{O}$ in the Heisenberg picture $\hat{O}(t) = e^{it\hat{H}'/\hbar}\hat{O}e^{-it\hat{H}'/\hbar}$ with the Hamiltonian $\hat{H}'$ after a quench. Both imaginary and real-time evolutions of MPSs in this study are performed with the time-evolving block decimation method [55–58] using the optimized Forest-Ruth-like decomposition [59]. Throughout this study, we set $w/J = 0.001$, the number of delocalized fermions N to nine, $L = 75$, $\tau = 1.0/J$, $n = 4$, and $\hat{H}_{\mathrm{even}}$ ($\hat{H}_{\mathrm{odd}}$) is the Hamiltonian linking even (odd) bonds of the Kondo model (1). On site terms are equally divided into $\hat{H}_{\mathrm{even}}$ and $\hat{H}_{\mathrm{odd}}$. The truncation error is set to 10^{-10} in imaginary-time evolution and 10^{-8} in real-time evolution, and the bond dimensions are allowed to increase up to 4000.

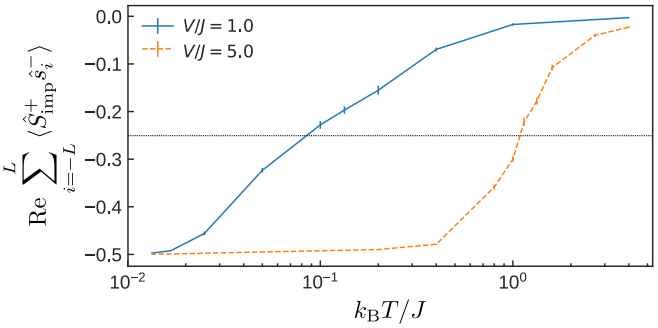

FIG. 2. The spin correlation versus temperature in steady states for $V/J = 1$ (blue solid line) and 5 (orange dashed line). Error bars indicate 1σ uncertainty. The horizontal dotted line represents $\mathrm{Re}\sum_i\langle\hat{S}^+_{\mathrm{imp}}\hat{s}^-_i\rangle = -0.25$, the criterion we used to define the Kondo temperature. We set $M = 0$ and $x_c = 0$.

Antiferromagnetic case.—We first consider the case that the spin-exchange interaction is antiferromagnetic and the total magnetization is zero, i.e., $V > 0$ and $M = \langle\hat{S}^z_{\mathrm{imp}} + \sum_i \hat{s}^z_i\rangle = 0$. In order to identify a temperature range in which the Kondo effect occurs, we show in Fig. 2 the spin correlation, $\mathrm{Re}\sum_i\langle\hat{S}^+_{\mathrm{imp}}\hat{s}^-_i\rangle = \sum_i\langle\hat{S}^x_{\mathrm{imp}}\hat{s}^x_i + \hat{S}^y_{\mathrm{imp}}\hat{s}^y_i\rangle$, for $V/J = 1$ (blue solid line) and 5 (orange dashed line), as a function of the temperature. It is clearly seen that when the temperature decreases, the spin correlation grows logarithmically, implying the formation of a many-body spin singlet.

From these spin correlations, we can extract an important energy scale called Kondo temperature T_K. At $T \lesssim T_K$, the spin-singlet correlation grows such that it makes significant contributions to physical quantities. In this Letter, we define the Kondo temperature as the temperature at which the spin correlation, $\mathrm{Re}\sum_i\langle\hat{S}^+_{\mathrm{imp}}\hat{s}_i\rangle$, becomes -0.25, namely, the half of the maximal singlet value. As discussed in the Supplemental Material [54], the Kondo temperatures given by this definition behave similar to the ordinary Kondo temperatures obtained by the perturbative renormalization group analysis [60], at least around $V/J = 1$. The Kondo temperature at $V/J = 1$ is around $0.1J/k_B$ and the estimated size of the Kondo screening cloud is around $10a$ [54,61]. In the following calculations for real-time dynamics at $V/J = 1$, we take $7.5 \le \beta J \le 75.0$, which corresponds approximately to $0.1 \le T/T_K \le 1$. Moreover, itinerant atoms are distributed over 40 sites (see Fig. 1), which is sufficiently larger than the Kondo screening length. Thus, our setting is adequate for observing the Kondo physics.

Notice that the Kondo temperature $T_K \sim 0.1J/k_B$ at V/J is remarkably lower than the lowest temperature, $T = 0.25J/k_B$, achieved in experiments with ultracold fermions [48]. We emphasize that the Kondo temperature can be

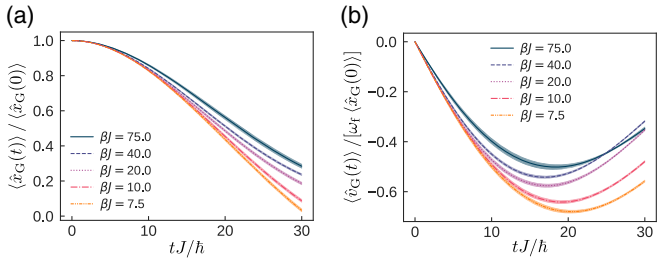

FIG. 3. Time evolution of the normalized c.m. (a) positions and (b) velocities for several temperatures. We set $V/J = 1$ and $M = 0$. The shaded regions are 1σ uncertainty of trajectories.

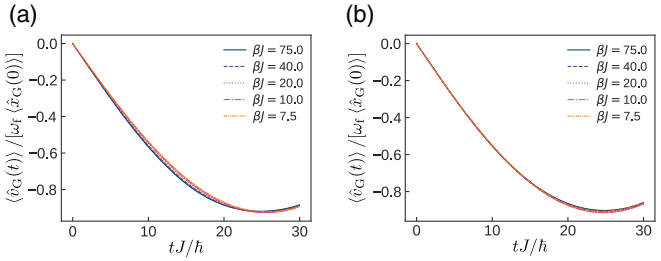

FIG. 4. Time evolution of the normalized c.m. velocities in the (a) fully spin-polarized system with $V/J = 1$ and in the (b) ferromagnetic Kondo model with $V/J = -1$.

significantly lifted by increasing V/J. For instance, Fig. 2 shows that T_K at $V/J = 5$ is well above $T = 0.25J/k_B$. Nevertheless, we set $V/J = 1$ for computations of real-time dynamics because the numerical cost is much more expensive for higher temperatures.

Figure 3 shows the time evolution of the c.m. positions and velocities at several temperatures after the shift of the trap center from $x_c = 3a$ to $x_c = 0$. The c.m. positions and velocities are, respectively, normalized by $\langle \hat{x}_G(0) \rangle$ and $\omega_f \langle \hat{x}_G(0) \rangle$, where $\omega_f = 2\sqrt{wJ}/\hbar$ denotes the dipole oscillation frequency of free particles [62]. $\omega_f \langle \hat{x}_G(0) \rangle$ means the maximum speed during the undamped dipole oscillation starting with the position $\langle \hat{x}_G(0) \rangle$. In Fig. 3, we see that the transport is significantly suppressed when the temperature decreases. This tendency is reminiscent of the Kondo effect, in which the resistance increases with a decrease in the temperature.

Fully spin-polarized and ferromagnetic cases.—In order to support our argument that the suppression of transport is a manifestation of the Kondo effect, we also compute the quench dynamics of the following two systems, which are widely known *not* to exhibit the Kondo effect [45]. The first example is a fully spin-polarized system ($M = 5$), in which the spin-exchange interaction term in Eq. (1) acts as a simple potential barrier term. In this system, we completely prohibit spin-flip processes that are essential for the Kondo effect [26]. Figure 4(a) represents the dynamics of the normalized c.m. velocities in the fully spin-polarized system. Except for the total magnetization M, any other settings are equivalent to those of the dynamics shown in Fig. 3. In contrast to the $M = 0$ case in Fig. 3(b), the normalized velocities in Fig. 4(a) do not show visible temperature dependence. This behavior is consistent with the formula of the resistance, $R \propto T^{2K-2}$, obtained from the Tomonaga-Luttinger (TL) liquid theory, where K denotes the Luttinger parameter for the charge sector and $K = 1$ for noninteracting fermions [63–66].

The second example is the case in which the spin-exchange interaction is ferromagnetic. Specifically, we take $V/J = -1$ and $M = 0$. Notice that, while there exists the ferromagnetic Kondo effect in 1D for $K < 1$ [45,67], this is not the case for noninteracting delocalized fermions considered here. This happens because they are also described by the TL liquid theory with $K = 1$. Figure 4(b) shows the time dependence of the normalized c.m. velocities in the ferromagnetic Kondo model. Except for the sign of V/J, any other settings are equivalent to the settings in Fig. 3. As in the fully spin-polarized case, the normalized c.m. velocities in the ferromagnetic Kondo model do not exhibit visible temperature dependence, and this is also consistent with $R \propto T^{2K-2}$.

In order to discuss the temperature dependence of the transport more quantitatively, we plot the quantity $\tilde{R} = 1 - \max_t |\langle \hat{v}_G(t) \rangle| / [\omega_f \langle \hat{x}_G(0) \rangle]$ in Fig. 5. As shown in the Supplemental Material [54], $\tilde{R}$ is approximately proportional to the resistance R under the assumption that $\tilde{R} \ll 1$ and is suited to characterizing the transport. In Fig. 5, we see that the temperature dependence of the transport is only visible in the antiferromagnetic Kondo model with spin-flip processes (blue solid line). We emphasize that the horizontal axis of Fig. 5 is logarithmic scale; $\tilde{R}$ of the antiferromagnetic Kondo model exhibits a logarithmic growth with a decrease in the temperature, which is a characteristic feature of the Kondo effect. Specifically, the "resistance" $\tilde{R}$ increases by around 1.7 times when the

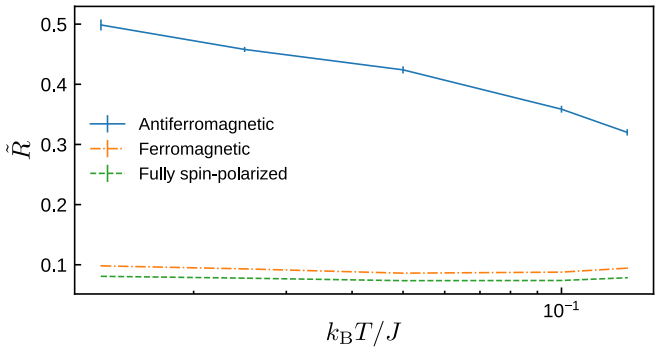

FIG. 5. Temperature dependence of $\tilde{R} = 1 - \max_t |\langle \hat{v}_G(t) \rangle| / (\omega_f \langle \hat{x}_G(0) \rangle)$. The solid, dashed, and dashed-dotted lines represent the antiferromagnetic Kondo ($M = 0$ and $V/J = 1$), fully spin-polarized ($M = 5$ and $V/J = 1$), and ferromagnetic Kondo ($M = 0$ and $V/J = -1$) systems. Error bars indicate 1σ uncertainty.

temperature decreases from $T \sim T_K$ to $0.1T_K$. Strictly speaking, we observe only the lower temperature side $0.1 \lesssim T/T_K \lesssim 1$ of the expected logarithmic dependence [68,69]. For the higher temperature side $1 \lesssim T/T_K \lesssim 10$, it requires a very expensive numerical cost. In this sense, corroborating the logarithmic dependence in the higher temperature region will be a suitable target of OLQS experiments. We suggest that observation of the logarithmic temperature dependence serves as a smoking-gun signature of the Kondo effect in the OLQS of the Kondo model.

Summary.—In order to propose an experimental way for observing the Kondo effect with ultracold alkaline-Earth-like atoms in optical lattices, we numerically simulated the finite-temperature dynamics of the one-dimensional Kondo model by using the quasiexact METTSs algorithm based on matrix product states. We found that when the spin-exchange interaction is antiferromagnetic, the c.m. motion after a sudden displacement of the trap potential is suppressed logarithmically with a decrease in the temperature. In contrast, it was shown that such suppression of the transport is absent in the ferromagnetic Kondo model or the fully spin-polarized system. These findings convincingly indicate that the Kondo effects in ultracold atoms are detectable via the simple transport measurement.

We also improved the numerical efficiency of the METTSs algorithm without breaking the total particle number conservation by the application of the Trotter gates. The modified METTSs algorithm can be applied to other systems for accurately analyzing static and dynamical properties at finite temperatures, such as the spectral functions [70] and the out-of-time ordered correlations [71].

We thank K. Ono and Y. Takahashi for fruitful discussions. The MPS calculations in this work are performed with ITensor library. This work was financially supported by KAKENHI from Japan Society for the Promotion of Science: Grants No. 18K03492 and No. 18H05228, by CREST, JST Grant No. JPMJCR1673, and by MEXT Q-LEAP Grant No. JPMXS0118069021.

*goto@phys.kindai.ac.jp
†danshita@phys.kindai.ac.jp

[1] F. Steglich, J. Aarts, C. D. Bredl, W. Lieke, D. Meschede, W. Franz, and H. Schäfer, Phys. Rev. Lett. **43**, 1892 (1979).
[2] G. R. Stewart, Rev. Mod. Phys. **56**, 755 (1984).
[3] L. M. Falicov and J. C. Kimball, Phys. Rev. Lett. **22**, 997 (1969).
[4] K. I. Kugel and D. I. Khomskii, Sov. Phys. JETP **52**, 501 (1980).
[5] Y. Tokura and N. Nagaosa, Science **288**, 462 (2000).
[6] Y. Kamihara, T. Watanabe, M. Hirano, and H. Hosono, J. Am. Chem. Soc. **130**, 3296 (2008).
[7] K. Kuroki, S. Onari, R. Arita, H. Usui, Y. Tanaka, H. Kontani, and H. Aoki, Phys. Rev. Lett. **101**, 087004 (2008).
[8] Q. Si, R. Yu, and E. Abrahams, Nat. Rev. Mater. **1**, 16017 (2016).
[9] T. Byrnes, N. Y. Kim, and Y. Yamamoto, Nat. Phys. **10**, 803 (2014).
[10] J. Kuneš, J. Phys. Condens. Matter **27**, 333201 (2015).
[11] R. P. Feynman, Int. J. Theor. Phys. **21**, 467 (1982).
[12] I. Bloch, J. Dalibard, and S. Nascimbène, Nat. Phys. **8**, 267 (2012).
[13] C. Gross and I. Bloch, Science **357**, 995 (2017).
[14] W. Hofstetter and T. Qin, J. Phys. B **51**, 082001 (2018).
[15] A. V. Gorshkov, M. Hermele, V. Gurarie, C. Xu, P. S. Julienne, J. Ye, P. Zoller, E. Demler, M. D. Lukin, and A. M. Rey, Nat. Phys. **6**, 289 (2010).
[16] M. Foss-Feig, M. Hermele, and A. M. Rey, Phys. Rev. A **81**, 051603(R) (2010).
[17] M. Nakagawa and N. Kawakami, Phys. Rev. Lett. **115**, 165303 (2015).
[18] R. Zhang, D. Zhang, Y. Cheng, W. Chen, P. Zhang, and H. Zhai, Phys. Rev. A **93**, 043601 (2016).
[19] Y. Cheng, R. Zhang, P. Zhang, and H. Zhai, Phys. Rev. A **96**, 063605 (2017).
[20] B. J. DeSalvo, M. Yan, P. G. Mickelson, Y. N. M. de Escobar, and T. C. Killian, Phys. Rev. Lett. **105**, 030402 (2010).
[21] T. Fukuhara, Y. Takasu, M. Kumakura, and Y. Takahashi, Phys. Rev. Lett. **98**, 030401 (2007).
[22] S. Taie, Y. Takasu, S. Sugawa, R. Yamazaki, T. Tsujimoto, R. Murakami, and Y. Takahashi, Phys. Rev. Lett. **105**, 190401 (2010).
[23] L. Riegger, N. D. Oppong, M. Höfer, D. R. Fernandes, I. Bloch, and S. Fölling, Phys. Rev. Lett. **120**, 143601 (2018).
[24] K. Ono, J. Kobayashi, Y. Amano, K. Sato, and Y. Takahashi, Phys. Rev. A **99**, 032707 (2019).
[25] M. Kitagawa, K. Enomoto, K. Kasa, Y. Takahashi, R. Ciuryło, P. Naidon, and P. S. Julienne, Phys. Rev. A **77**, 012719 (2008).
[26] J. Kondo, Prog. Theor. Phys. **32**, 37 (1964).
[27] A. A. Abrikosov, Phys. Phys. Fiz. **2**, 5 (1965).
[28] K. Yosida, Phys. Rev. **147**, 223 (1966).
[29] P. W. Anderson, J. Phys. C **3**, 2436 (1970).
[30] K. G. Wilson, Rev. Mod. Phys. **47**, 773 (1975).
[31] N. Andrei, K. Furuya, and J. H. Lowenstein, Rev. Mod. Phys. **55**, 331 (1983).
[32] S. Doniach, Physica (Amsterdam) **91B+C**, 231 (1977).
[33] S. Burger, F. S. Cataliotti, C. Fort, F. Minardi, M. Inguscio, M. L. Chiofalo, and M. P. Tosi, Phys. Rev. Lett. **86**, 4447 (2001).
[34] C. D. Fertig, K. M. O'Hara, J. H. Huckans, S. L. Rolston, W. D. Phillips, and J. V. Porto, Phys. Rev. Lett. **94**, 120403 (2005).
[35] N. Strohmaier, Y. Takasu, K. Günter, R. Jördens, M. Köhl, H. Moritz, and T. Esslinger, Phys. Rev. Lett. **99**, 220601 (2007).
[36] D. McKay, M. White, M. Pasienski, and B. DeMarco, Nature (London) **453**, 76 (2008).
[37] E. Haller, R. Hart, M. J. Mark, J. G. Danzl, L. Reichsöllner, M. Gustavsson, M. Dalmonte, G. Pupillo, and H.-C. Nägerl, Nature (London) **466**, 597 (2010).
[38] L. Tanzi, S. Scaffidi Abbate, F. Cataldini, L. Gori, E. Lucioni, M. Inguscio, G. Modugno, and C. D'Errico, Sci. Rep. **6**, 25965 (2016).
[39] G. Boéris, L. Gori, M. D. Hoogerland, A. Kumar, E. Lucioni, L. Tanzi, M. Inguscio, T. Giamarchi, C. D'Errico,

G. Carleo, G. Modugno, and L. Sanchez-Palencia, Phys. Rev. A **93**, 011601(R) (2016).
[40] S. R. White, Phys. Rev. Lett. **69**, 2863 (1992).
[41] S. R. White, Phys. Rev. B **48**, 10345 (1993).
[42] U. Schollwöck, Ann. Phys. (Amsterdam) **326**, 96 (2011).
[43] S. R. White, Phys. Rev. Lett. **102**, 190601 (2009).
[44] E. M. Stoudenmire and S. R. White, New J. Phys. **12**, 055026 (2010).
[45] A. Furusaki, J. Phys. Soc. Jpn. **74**, 73 (2005).
[46] T. Kasuya, Prog. Theor. Phys. **16**, 45 (1956).
[47] M. F. Parsons, A. Mazurenko, C. S. Chiu, G. Ji, D. Greif, and M. Greiner, Science **353**, 1253 (2016).
[48] A. Mazurenko, C. S. Chiu, G. Ji, M. F. Parsons, M. Kanász-Nagy, R. Schmidt, F. Grusdt, E. Demler, D. Greif, and M. Greiner, Nature (London) **545**, 462 (2017).
[49] F. Verstraete, J. J. García-Ripoll, and J. I. Cirac, Phys. Rev. Lett. **93**, 207204 (2004).
[50] A. E. Feiguin and S. R. White, Phys. Rev. B **72**, 220401(R) (2005).
[51] M. Binder and T. Barthel, Phys. Rev. B **92**, 125119 (2015).
[52] S. Goto and I. Danshita, Phys. Rev. A **96**, 063602 (2017).
[53] M. Binder and T. Barthel, Phys. Rev. B **95**, 195148 (2017).
[54] See Supplemental Material at http://link.aps.org/supplemental/10.1103/PhysRevLett.123.143002 for the validity and some benchmark results of our improved method, the comparison of the Kondo temperatures we define and the ordinary perturbative one, and the derivation of the relation between the resistance R and the quantity $\tilde{R}$.
[55] G. Vidal, Phys. Rev. Lett. **91**, 147902 (2003).
[56] G. Vidal, Phys. Rev. Lett. **93**, 040502 (2004).
[57] S. R. White and A. E. Feiguin, Phys. Rev. Lett. **93**, 076401 (2004).
[58] A. J. Daley, C. Kollath, U. Schollwöck, and G. Vidal, J. Stat. Mech. (2004) P04005.
[59] I. P. Omelyan, I. M. Mryglod, and R. Folk, Comput. Phys. Commun. **146**, 188 (2002).
[60] A. C. Hewson, *The Kondo Problem to Heavy Fermions* (Cambridge University Press, Cambridge, England, 1997).
[61] E. S. Sørensen and I. Affleck, Phys. Rev. B **53**, 9153 (1996).
[62] A. M. Rey, Ultracold Bosonic Atoms in Optical Lattices, Ph.D. thesis, University of Maryland, 2004.
[63] C. L. Kane and M. P. A. Fisher, Phys. Rev. B **46**, 15233 (1992).
[64] Y. Kagan, N. V. Prokof'ev, and B. V. Svistunov, Phys. Rev. A **61**, 045601 (2000).
[65] H. P. Büchler, V. B. Geshkenbein, and G. Blatter, Phys. Rev. Lett. **87**, 100403 (2001).
[66] I. Danshita, Phys. Rev. Lett. **111**, 025303 (2013).
[67] A. Furusaki and N. Nagaosa, Phys. Rev. Lett. **72**, 892 (1994).
[68] T. A. Costi, Phys. Rev. Lett. **85**, 1504 (2000).
[69] L. Merker, S. Kirchner, E. Muñoz, and T. A. Costi, Phys. Rev. B **87**, 165132 (2013).
[70] E. Coira, P. Barmettler, T. Giamarchi, and C. Kollath, Phys. Rev. B **98**, 104435 (2018).
[71] A. Bohrdt, C. B. Mendl, M. Endres, and M. Knap, New J. Phys. **19**, 063001 (2017).